International Journal of Minerals, Metallurgy and Materials
Volume 18, Number 4, August 2011, Page 430
DOI: 10.1007/s12613-011-0458-1

Effects of aging on the microstructure of a Cu-Al-Ni-Mn shape memory alloy

U. Sari[1)], *T. Kirindi*[2)], *F. Ozcan*[3)], *and M. Dikici*[4)]

1) Department of Elementary Education, Elementary Science Education, Kirikkale University, Kirikkale 71450, Turkey
2) Department of Computer Education and Instructional Technology, Kirikkale University, Kirikkale 71450, Turkey
3) Institute of Sciences, Kirikkale University, Kirikkale 71450, Turkey
4) Department of Physics, Kirikkale University, Kirikkale 71450, Turkey
(Received: 21 May 2010; revised: 6 July 2010; accepted: 12 July 2010)

Abstract: The influence of aging on the microstructure and mechanical properties of Cu-11.6wt%Al-3.9wt%Ni-2.5wt%Mn shape memory alloy (SMA) was studied by means of scanning electron microscopy (SEM), transmission electron microscopy (TEM), X-ray diffractometer, and differential scanning calorimeter (DSC). Experimental results show that bainite, γ_2, and α phase precipitates occur with the aging effect in the alloy. After aging at 300°C, the bainitic precipitates appear at the early stages of aging, while the precipitates of γ_2 phase are observed for a longer aging time. When the aging temperature increases, the bainite gradually evolves into γ_2 phase and equilibrium α phase (bcc) precipitates from the remaining parent phase. Thus, the bainite, γ_2, and α phases appear, while the martensite phase disappears progressively in the alloy. The bainitic precipitates decrease the reverse transformation temperature while the γ_2 phase precipitates increase these temperatures with a decrease of solute content in the retained parent phase. On the other hand, these precipitations cause an increasing in hardness of the alloy.

Keywords: copper alloys; shape memory effect; martensitic transformations; aging; precipitates

1. Introduction

Cu-based shape memory alloys (SMAs) are commercially attractive alloys for practical applications owing to their low cost and relative ease of processing together with a reasonable shape memory effect. Among Cu-based SMAs, CuAlNi alloys are popular due to their wide range of useful transformation temperature and small hysteresis. They are also the only SMAs that can be used at temperatures near 200°C, which is the advantage over CuZnAl and TiNi alloys whose maximum working temperatures are about 100°C [1-2].

Although Cu-Al-Ni SMAs have a better thermal stability and a higher operating temperature, their practical applications are highly restricted by very small shape changes due to their poor workability and susceptibility to brittle intergranular cracks [3]. Their very high elastic anisotropy and large grain sizes cause brittle and poor mechanical properties owing to the high degree of order in the parent phase with B2, DO_3 or $L2_1$ structure. Adding some alloying elements such as Mn, Ti, Fe, Zr, and B to the alloys can significantly improve their ductility and properly modify their operating temperatures [4-9]. Particularly, Mn addition in the alloys has been proved to enhance the thermoelastic and pseudoelastic behaviors [6].

β-phases in Cu-Al-Ni SMAs have A2-type disordered structures at high temperature and undergo the ordered structures with B2-, DO_3-, or $L2_1$-type superlattices during quenching from high temperature. These ordered structures also transform into close-packet martensite structures (6R, 18R, and 2H; R rhombohedral and H hexagonal) with further cooling [10-11]. On the other hand, the characteristics of martensitic transformations are very sensitive to the order degree of β phase and the precipitate process of the stable phase due to the metastable character of this phase [9,12-13]. In addition, the precipitation and the aging phenomena become dominant in the alloys when they are used at high

Corresponding author: U. Sari E-mail: usari05@yahoo.com

temperature.

The origin of aging effect in Cu-Al-Ni SMAs is rather complex. It is known that the aging process, either in the state of parent or martensite phase, is a complicated thermally activated diffusional process, in which atom rearrangement occurs. It is believed that the changes in the state of atomic order will play a key part in aging effect [8]. On the other hand, upon aging in the parent phase of Cu-Al-Ni SMAs at elevated temperatures, the precipitation of equilibrium phases (α and γ_2 type) is expected to take place as a result of decomposition of the metastable parent phase β [14-16]. The precipitation phases considerably affect martensitic and reverse transformations, and thus, the characteristic of shape memory effect changes in the alloys.

In the present work, the effects of aging in the state of parent phase on the microstructure and mechanical properties of Cu-11.6wt%Al-3.9wt%Ni-2.5wt%Mn alloy have been investigated by means of scanning electron microscopy (SEM), transmission electron microscopy (TEM), X-ray diffractometer, and differential scanning calorimeter (DSC).

2. Experimental procedures

The alloy used for this study was prepared by melting the pure elements (99.9%) in an argon atmosphere and quenching as-cylindrical rods with a size of ϕ1 cm×10 cm. The chemical composition of the alloy was obtained as Cu-11.6wt%Al-3.9wt%Ni-2.5wt%Mn by using the electron dispersion spectroscopy technique. Special samples from the ingot alloy were cut by a diamond saw. Samples were sealed into quartz tubes and then heat-treated in the β-phase equilibrium region. They were homogenized at 950°C for 2 h followed by quenching into iced water. Aging of the samples was produced by isothermal holding at various temperatures from 300 to 500°C and then quenched in a water bath at room temperature. In addition, the alloy was aged at 300°C for different intervals of time.

For SEM observations, the surfaces of the specimens were first mechanically polished, and afterwards, the damaged surface layers were eliminated by etching in a solution composed of 2.5 g $FeCl_3 \cdot 6H_2O$, 48 mL methanol, and 10 mL HCl for 4 min. SEM observations were made in a JEOL 5600 scanning microscope operated at 20 kV. Samples for TEM observations were prepared from the heat-treated specimens. Discs of about 0.4 mm in thickness were cut from the samples with a low-speed diamond saw and then thinned to 0.1 mm with 800 and 1200 grit emery papers and punched into 3-mm diameter discs. Finally, these discs were prepared by double jet electro-polishing in a Streurs-Tenupol jet unit with a solution of 30vol% HNO_3-70vol% methanol at −10°C and 10 V. TEM observations were performed by a JEOL 3010 electron microscope operated at 300 kV with a double tilt specimen. In addition, X-ray measurements were carried out using a Rigaku Geigerflex D-MaxB X-ray diffractometer with Cu K_α radiation. The transformation characteristics of the alloy were examined by DSC. The DSC measurements were made with a Perkin-Elmer Sapphire model thermal analyzer at 25-300°C with a heating rate of 10°C/min. Microhardness measurements were performed by a Type BMS 200-RB, and the measurements were given in Brinell. Each hardness value was obtained as the average of at least three measurements on a surface.

3. Results

3.1. Microstructure of the as-quenched alloy

To obtain information of the microstructure and the crystal structure of the thermally-induced martensite, SEM and TEM observations and X-ray analysis of the quenched specimen were carried out (Fig. 1). Fig. 1(a) shows the SEM micrograph of the as-quenched alloy. The alloy is in martensitic state at room temperature. The grains appear clearly, and

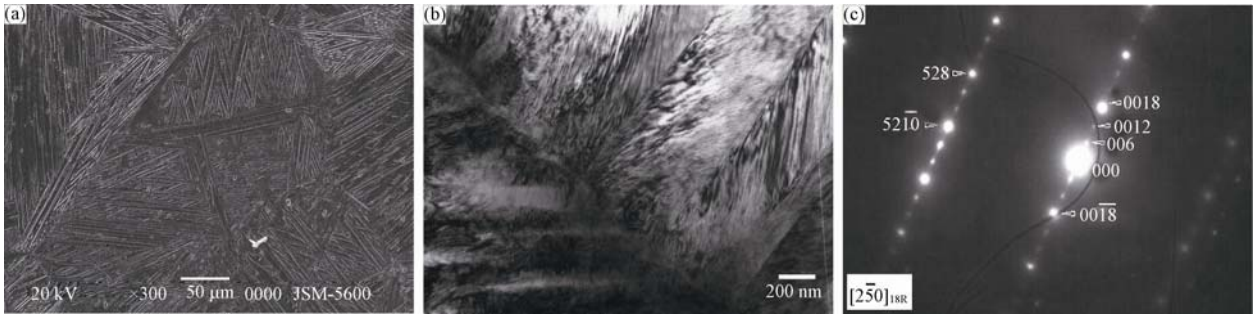

Fig. 1. SEM and TEM images of the alloy: (a) SEM image showing the microstructure of the alloy; (b) bright field electron micrograph of the martensite structure; (c) selected area electron diffraction pattern.

martensite plates have different orientations in different grains. It is obviously that martensite appears in the typical self-accommodating zig-zag morphology of β_1' martensite. The β_1' variants are small and have a highly thermoelastic behavior due to their controlled growth in self-accommodating groups [12, 17]. Fig. 1(a) indicates also that the microstructure of martensite consists of self-accommodating plate groups, and different plate groups are present at the same parent phase grain. Martensite plate groups nucleate at numerous sites in the grain, and the martensite growth process involves the accommodation of local stress fields that require the formation of other plate groups [18].

Fig. 1(b) shows a TEM image of the martensite microstructure in the Cu-Al-Ni-Mn alloy. Here, two different groups of the parallel plates separating from one another with the grain boundary are seen. The martensite plate group comprises twinned martensite laths with two kinds of self-accommodating variants, and the striations in each variant are the basal-stacking faults. According to the analysis of the selected area diffraction pattern taken from the martensite variant, the stacking sequence of the martensite structure is 18R (Fig. 1(c)). The stacking order in the pattern has also a three-layer period for the 18R martensite with the $[2\bar{5}0]$ orientation. On the other hand, careful observation of the alloy by TEM shows no evidence of γ_1' martensite (2H stacking sequence) formation.

Fig. 2 shows an X-ray profile of the as-quenched alloy. Here, it can be seen that the as-quenched alloy consists of monoclinic M18R martensite and exhibits superlattice reflections. According to the diffractogram, the martensite phase is an ordered case, and sublattices are occupied regularly by certain atoms with different atomic sizes. The martensite basal plane $(110)_\beta$ undergoes a hexagonal distortion due to the difference in atom size. Due to the distortion, the spacing differences between particularly selected pairs of diffraction planes providing a special relation between miller indices (h and k) become different from zero and can reflect the order degree of martensite. This relation is given as $\frac{h_1^2 - h_2^2}{3} = \frac{k_2^2 - k_1^2}{n}$, where n is 4 for the 18R martensite [19]. The plane pairs providing the relation can be listed as $12\bar{2}$ - 202 , $12\bar{8}$ - 208 , and 041-320.

3.2. Aging in the parent phase

Fig. 3 shows the microstructure after aging at 300°C for different periods and various temperatures. As seen in Fig. 3(a), no change of the morphology of martensite plates can be seen in the early stage of aging. On the other hand, some martensite plates are seemingly distorted. After aging at 300°C for 2 h, thin bainite precipitates are clearly observed (Fig. 3(b)). After a long period aging, typical chevron-shaped bainite plates dominate, as shown in Fig. 3(c). Besides, some γ_2 precipitates are seen in Fig. 3(c). When the aging temperature increases, bainite gradually evolves into γ_2 phase and equilibrium α phase precipitates from the remaining parent phase (Figs. 3(d) and (e)). As seen in Fig. 3(d), the new phase precipitates (γ_2 phase) commonly appear in grain boundaries by aging at 400°C. Thus, the martensite ratio decreases in favor of the phase precipitates. In Fig. 3(e), the parent phase completely decomposes into disorder equilibrium phases α and γ_2.

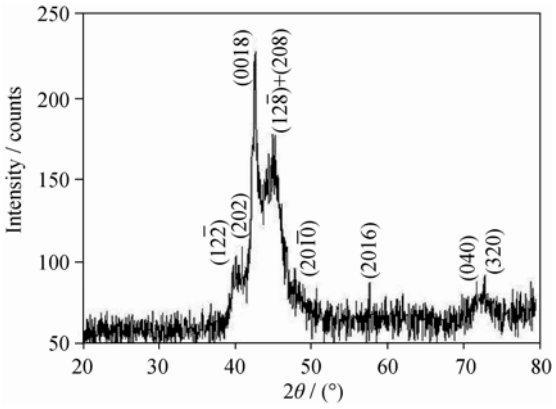

Fig. 2. X-ray profile of the as-quenched alloy.

Fig. 4 shows XRD profiles measured at room temperature of the alloy after aging at different temperatures and periods. The X-ray profiles are almost similar for the as-quenched alloy and aged samples at 300°C with different periods. The X-ray diffraction of the alloy aged at 300°C for 24 h exhibits peaks corresponding to bainitic and γ_2 precipitates. The bainite may possess either the M18R- or M9R-type order structure, depending on the order type in the parent phase [8]. Therefore, the XRD profiles of the bainite and martensite structures are coherent with each other, as seen in Fig. 4. However, intensities of the martensite peaks decrease, while the $(220)_\beta$ peak becomes more intense, and the (300) peak of the γ_2 phase appears in Fig. 4(e). This peak shows that γ_2 phase precipitates in small amount occur after aging at 300°C for 24 h. The parent phase gives a complex structure, a mixture of equilibrium and non-equilibrium phases after aging at 400°C. While the martensite peaks progressively disappear, and the peaks of γ_2 and α phases appear. Particularly, the intensity of the (300) peak of γ_2 increases with the aging temperature rising. This increase in γ_2 phase is also seen clearly in Fig. 3(d). Fig. 4(f) reveals that the

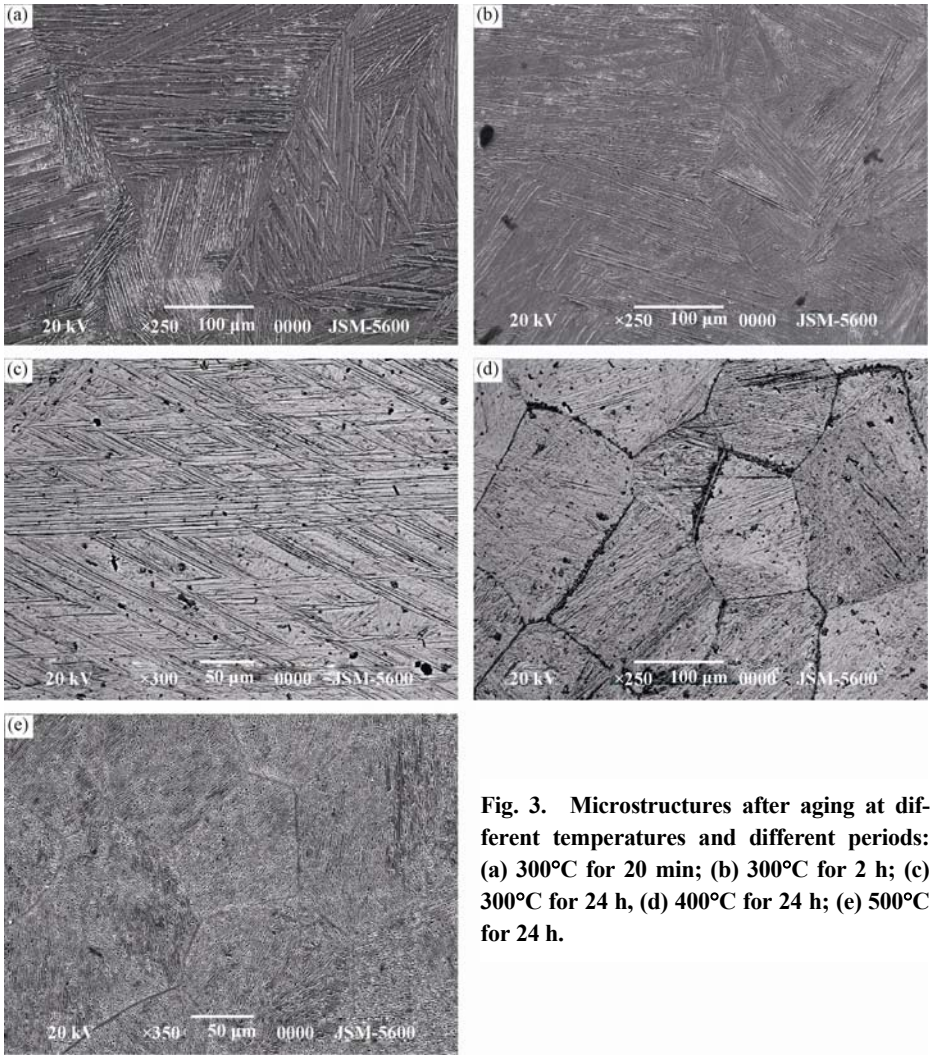

Fig. 3. Microstructures after aging at different temperatures and different periods: (a) 300°C for 20 min; (b) 300°C for 2 h; (c) 300°C for 24 h, (d) 400°C for 24 h; (e) 500°C for 24 h.

parent phase does not transform to martensite and completely decomposes into disorder equilibrium phases α and γ_2.

Aging effects on the transformation characteristic of the alloy have been evaluated with the aid of DSC. Fig. 5 shows the DSC scans of the as-quenched and aged samples. In the early stage of aging, the reverse transformation temperatures increase upon aging at 300°C for 20 min. This change can be attributed to atomic reordering. The aging causes an increase in order degree of the parent phase, and thus, the transformation temperatures increase [8]. After aging at 300°C for 2 h, the reverse transformation temperatures slowly decrease due to the formation of bainite. The formation of bainite causes an increase in the content of solute atoms in the retained parent phase, and the transformation temperatures decrease usually with the increase. After longer periods, aging at 300°C for 24 h, the precipitates of the solute-rich γ_2 phase lead to the decrease of solute content in the parent phase, and thus, the transformation temperatures increase as seen in Fig. 5. In addition, the transformation temperatures increase due to the formation of γ_2 phase precipitation after aging at 400°C. The parent phase totally decomposes into equilibrium phases α and γ_2 with aging at 500°C. Therefore, the reverse transformation is not observed in Fig. 5.

The variation of Brinell hardness as a function of aging temperature and time is given in Fig. 6. Besides, the hardness value of the as-quenched alloy was measured as HB_{10} 118 on the Brinell hardness scale. Fig. 6(a) shows that the hardness slowly increases with an increase in aging time. This increase in hardness stems from the precipitation of bainite, and it reveals an increase in the amount of bainite with increasing aging time. Besides, the hardness significantly increases with the increase of aging temperature. This result stems from the precipitation of γ_2 and α phases. As seen in

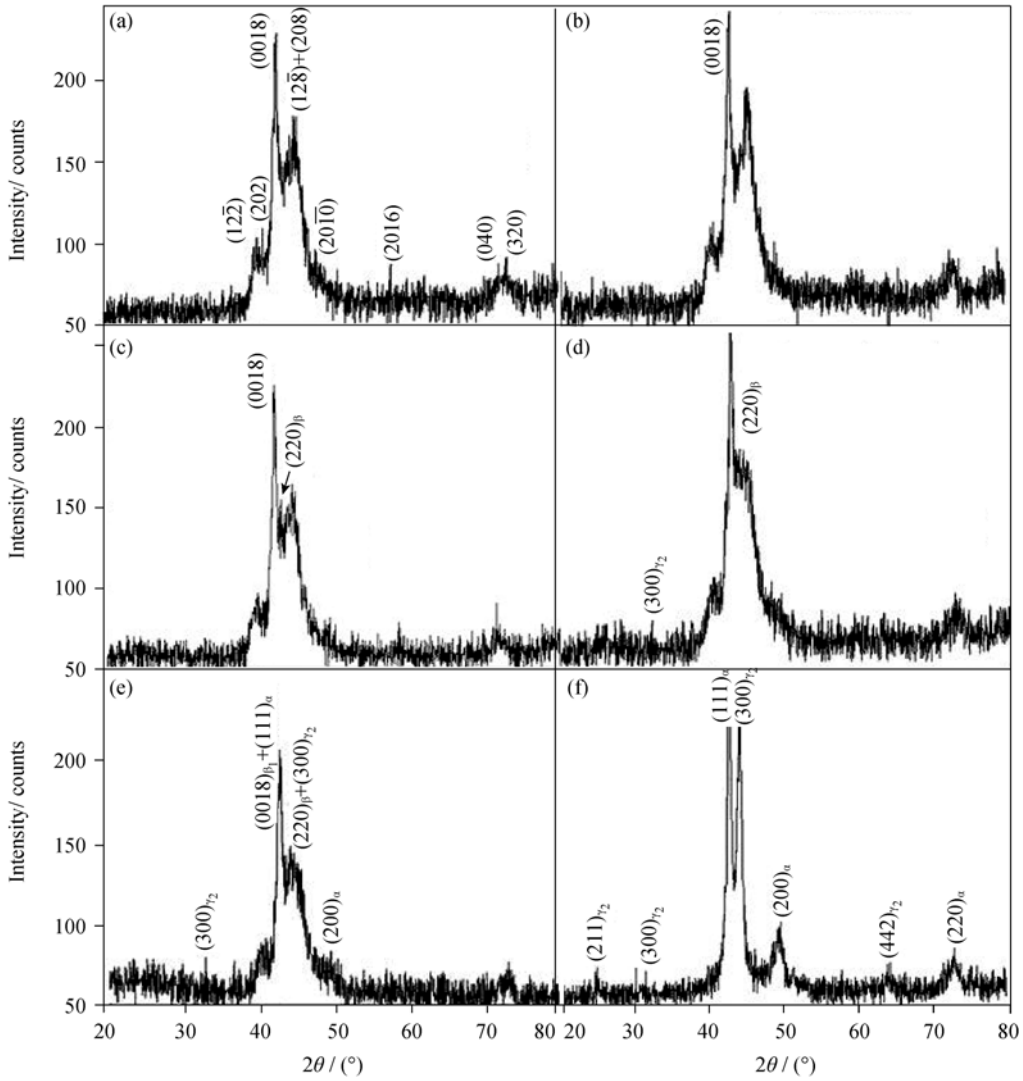

Fig. 4. XRD profiles of the alloy after aging at different temperatures and periods: (a) as-quenched; (b) 300°C for 20 min., (c) 300°C for 2 h; (d) 300°C for 24 h; (e) 400°C for 24 h; (f) 500°C for 24 h.

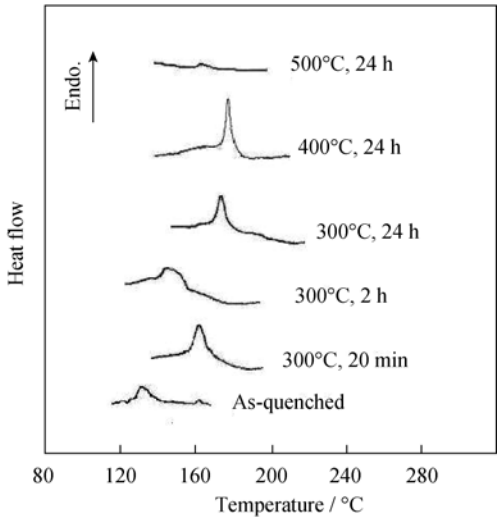

Fig. 5. DSC scans of the as-quenched and aged samples.

Figs. 3 and 4, the amount of precipitate phases increases with the increase of aging temperature, and thus, the hardness also increases. In addition, the hardness of the as-quenched alloy in the martensite state is smaller than that of the aged samples. It shows that the precipitate phases are harder than the martensite phase.

4. Discussion

The CuAlNi alloys are only SMAs that can be used at high temperature. Therefore, it is important to know the effects of thermal treatment at high temperature on the alloys. In these alloys, the precipitation and the aging phenomena become dominant at high temperature. In addition, the martensitic transformations have a diffusionless character, and the configuration and structural defects in the β-phase

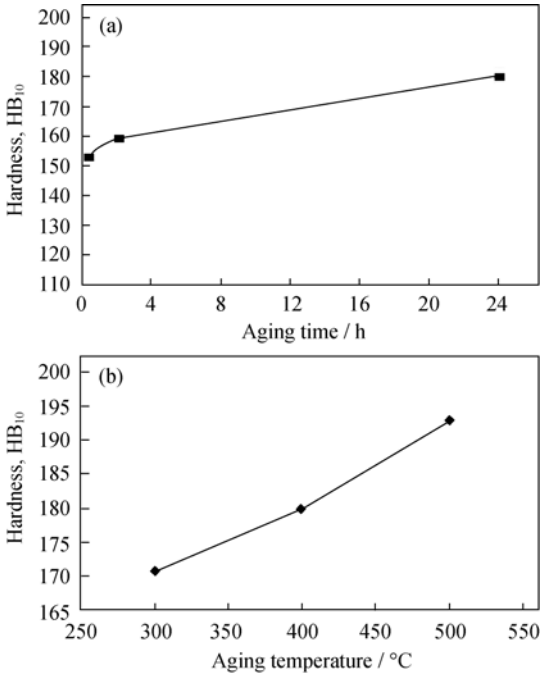

Fig. 6. Brinell hardness as a function of aging time (a) and temperature (b).

inherit to martensite phase. Hence, any change in the physical property of the β-phase corresponds with the change in the same property of martensite. Consequently, the mechanic and thermodynamic properties of the alloys such as shape memory effect, pseudoelasticity, and rubber-like behavior can be changed significantly with heat treatment.

The present work shows that the microstructure and transformation characteristics of the alloy considerably change with aging. This change stems from the occurrence of bainite, γ_2 phase, and α phase precipitates and atomic order. These phases affect also the shape memory behavior of the alloy. The bainitic precipitates appear at the early stages of aging, while the precipitates of γ_2 and α phases are observed for a longer aging time at higher temperatures. In Cu-based SMAs, it is well known that the bainite phase is poor in alloying elements, while precipitation of the γ_2 phase is rich. Therefore, the content of alloying elements in the parent phase changes when the alloy aged at high temperature. The transformation temperatures are very sensitive to these small variations in the alloy composition. Consequently, the bainitic precipitate decreases the reverse transformation temperature with the content of solute atoms increasing, whereas the γ_2 phase precipitates increase with the decrease of solute content in the retained parent phase.

The formation of bainite decreases also the amount of the thermoelastic martensite since the bainitic transformation is irreversible. Thus, it causes a degradation of shape memory effect of the alloy. In addition, the parent phase totally decomposes into equilibrium phases α and γ_2 with aging at 500°C. In this case, the reverse transformation does not occur in the alloy, and thus, the shape memory effect disappears. On the other hand, the hardness of the alloy increases with aging. These results display that the CuAlNiMn alloy is more susceptible to aging effect.

5. Conclusion

The effects of aging in the parent phase state on the microstructure and mechanical properties of Cu-11.6wt% Al-3.9wt%Ni-2.5wt%Mn alloy were investigated by means of SEM, TEM, X-ray diffractometer, and DSC. The results show that the aging considerably influences the microstructure, the reverse transformation temperatures, and the mechanical properties of the alloy. Bainitic precipitation appears at the early stages of aging, while the precipitates of γ_2 and α phases are observed for a longer aging time at higher temperature. The bainitic precipitates decrease the reverse transformation temperature with the content of solute atoms increasing, while γ_2 phase precipitates increase with the decrease of solute content in the retained parent phase. On the other hand, these precipitates cause an increase in hardness of the alloy.

References

[1] J.I. Pérez-Landazábal, V. Recarte, V. Sánchez-Alarcos, *et al*., Study of the stability and decomposition process of the β phase in Cu-Al-Ni shape memory alloys, *Mater. Sci. Eng. A*, 438-440(2006), p.734.

[2] G. Zak, A.C. Kneissl, and G. Zatulskij, Shape memory effect in cryogenic Cu-Al-Mn alloys, *Scripta Mater*., 34(1996), p.363.

[3] Z.G. Wei, H.Y. Peng, D.Z. Yang, *et al*., Reverse transformations in CuAlNiMnTi alloy at elevated temperatures, *Acta Mater*., 44(1996), p.1189.

[4] M.A. Morris, Influence of boron additions on ductility and microstructure of shape memory Cu-Al-Ni alloys, *Scripta Metall. Mater*., 25(1991), p.2541.

[5] M.A. Morris, High temperature properties of ductile Cu-Al-Ni shape memory alloys with boron additions, *Acta Metall. Mater*., 40(1992), p.1573.

[6] M.A. Morris and T. Lipe, Microstructural influence of Mn additions on thermoelastic and pseudoelastic properties of Cu-Al-Ni alloys, *Acta Metall. Mater*., 42(1994), p.1583.

[7] K. Adachi, K. Shoji, and Y. Hamada, Formation of X phases and origin of grain refinement effect in Cu-Al-Ni shape memory alloys added with titanium, *ISIJ Int*., 29(1989),

p.378.

[8] Z.G. Wei, H.Y. Peng, W.H. Zou, and D.Z. Yang, Aging effects in a Cu-12Al-5Ni-2Mn-1Ti shape memory alloy, *Metall. Mater. Trans. A*, 28(1997), p.955.

[9] U. Sari, Influences of 2.5wt% Mn addition on the microstructure and mechanical properties of Cu-Al-Ni shape memory alloys, *Int. J. Miner. Metall. Mater.*, 17(2010), No.2, p.192.

[10] S. Miyazaki and K. Otsuka, Development of shape memory alloys, *ISIJ Int*., 29(1989), p.353.

[11] T. Saburi and C.M. Wayman, Crystallographic similarities in shape memory martensites, *Acta Metall*., 27(1979), p.979.

[12] U. Sari and I. Aksoy, Electron microscopy study of 2H and 18R martensites in Cu-11.92wt% Al-3.78wt% Ni shape memory alloy, *J. Alloys Compd*., 417(2006), p.138.

[13] U. Sari and T. Kirindi, Effects of deformation on microstructure and mechanical properties of a Cu-Al-Ni shape memory alloy, *Mater. Charact*., 59(2008), p.920.

[14] H. Cheniti, M. Bouabdallah, and E. Patoor, High temperature decomposition of the β_1 phase in a Cu-Al-Ni shape memory alloy, *J. Alloys Compd*., 476(2009), p.420.

[15] W. Zou, J. Gui, R. Wang, *et al*., Bainitic precipitation and its effect on the martensitic transformation in the Cu-Al-Ni-Mn-Ti shape-memory alloy, *J. Mater. Sci*., 32(1997), p.5279.

[16] N. Suresh and U. Ramamurty, Effect of aging on mechanical behavior of single crystal Cu-Al-Ni shape memory alloys, *Mater. Sci. Eng. A*, 454-455(2007), p.492.

[17] V. Recarte, R.B. Pérez-Sáez, E.H. Bocanegra, *et al*., Influence of Al and Ni concentration on the martensitic transformation in Cu-Al-Ni shape-memory alloys, *Metall. Mater. Trans. A*, 33(2002), p.2581.

[18] U. Sari and I. Aksoy, Micro-structural analysis of self-accommodating martensites in Cu-11.92wt% Al-3.78wt% Ni shape memory alloy, *J. Mater. Process. Technol*., 195(2008), p.72.

[19] A. Aydogdu, Y. Aydogdu, and O. Adiguzel, Long-term ageing behaviour of martensite in shape memory Cu-Al-Ni alloys, *J. Mater. Process. Technol*., 153-154(2004), p.164.